Dielectron production in Ar + KCl collisions at 1.76A GeV

G. Agakishiev,[6] A. Balanda,[3] D. Belver,[16] A. Belyaev,[6] A. Blanco,[2] M. Böhmer,[12] J. L. Boyard,[14] P. Cabanelas,[16] E. Castro,[16]
S. Chernenko,[6] T. Christ,[12] M. Destefanis,[8] F. Dohrmann,[5] A. Dybczak,[3] T. Eberl,[12] E. Epple,[11] L. Fabbietti,[11] O. Fateev,[6]
P. Finocchiaro,[1] P. Fonte,[2,*] J. Friese,[12] I. Fröhlich,[7] T. Galatyuk,[7,†] J. A. Garzón,[16] R. Gernhäuser,[12] C. Gilardi,[8]
M. Golubeva,[10] D. González-Díaz,[4,‡] F. Guber,[10] M. Gumberidze,[14] T. Heinz,[4] T. Hennino,[14] R. Holzmann,[4,§] P. Huck,[12]
I. Iori,[9,∥] A. Ivashkin,[10] M. Jurkovic,[12] B. Kämpfer,[5,¶] K. Kanaki,[5] T. Karavicheva,[10] I. Koenig,[4] W. Koenig,[4] B. W. Kolb,[4]
R. Kotte,[5] A. Krása,[15] F. Krizek,[15] R. Krücken,[12] H. Kuc,[3,14] W. Kühn,[8] A. Kugler,[15] A. Kurepin,[10] S. Lang,[4] J. S. Lange,[8]
K. Lapidus,[10,11] T. Liu,[14] L. Lopes,[2] M. Lorenz,[7] L. Maier,[12] A. Mangiarotti,[2] J. Markert,[7] V. Metag,[8] B. Michalska,[3]
J. Michel,[7] E. Morinière,[14] J. Mousa,[13] C. Müntz,[7] L. Naumann,[5] J. Otwinowski,[3] Y. C. Pachmayer,[7] M. Palka,[7] V. Pechenov,[4]
O. Pechenova,[7] J. Pietraszko,[7] W. Przygoda,[3] B. Ramstein,[14] A. Reshetin,[10] A. Rustamov,[4] A. Sadovsky,[10] B. Sailer,[12]
P. Salabura,[3] A. Schmah,[11,**] E. Schwab,[4] J. Siebenson,[11] Yu. G. Sobolev,[15] S. Spataro,[8,††] B. Spruck,[8] H. Ströbele,[7] J.
Stroth,[7,4] C. Sturm,[4] A. Tarantola,[7] K. Teilab,[7] P. Tlusty,[15] M. Traxler,[4] R. Trebacz,[3] H. Tsertos,[13] V. Wagner,[15] M. Weber,[12]
C. Wendisch,[5] M. Wisniowski,[3] J. Wüstenfeld,[5] S. Yurevich,[4] and Y. Zanevsky[6]

(HADES Collaboration)

[1]*Istituto Nazionale di Fisica Nucleare-Laboratori Nazionali del Sud, I-95125 Catania, Italy*
[2]*LIP-Laboratório de Instrumentação e Física Experimental de Partículas, P-3004-516 Coimbra, Portugal*
[3]*Smoluchowski Institute of Physics, Jagiellonian University of Cracow, PL-30-059 Kraków, Poland*
[4]*GSI Helmholtzzentrum für Schwerionenforschung GmbH, D-64291 Darmstadt, Germany*
[5]*Institut für Strahlenphysik, Forschungszentrum Dresden Rossendorf, D-01314 Dresden, Germany*
[6]*Joint Institute of Nuclear Research, RU-141980 Dubna, Russia*
[7]*Institut für Kernphysik, Goethe-Universität, D-60438 Frankfurt, Germany*
[8]*II.Physikalisches Institut, Justus Liebig Universität Giessen, D-35392 Giessen, Germany*
[9]*Istituto Nazionale di Fisica Nucleare, Sezione di Milano, I-20133 Milano, Italy*
[10]*Institute for Nuclear Research, Russian Academy of Science, 117312 Moscow, Russia*
[11]*Excellence Cluster "Origin and Structure of the Universe," D-85748 München, Germany*
[12]*Physik Department E12, Technische Universität München, D-85748 München, Germany*
[13]*Department of Physics, University of Cyprus, 1678 Nicosia, Cyprus*
[14]*Institut de Physique Nucléaire (UMR 8608), CNRS/IN2P3-Université Paris Sud, F-91406 Orsay Cedex, France*
[15]*Nuclear Physics Institute, Academy of Sciences of Czech Republic, CZ-25068 Rez, Czech Republic*
[16]*Departamento de Física de Partículas, Univ. de Santiago de Compostela, E-15706 Santiago de Compostela, Spain*

We present results on dielectron production in ^{40}Ar + KCl collisions at 1.76A GeV. For the first time ω mesons could be reconstructed in a heavy-ion reaction at a bombarding energy which is well below the production threshold in free nucleon-nucleon collisions. The ω multiplicity has been extracted and compared to the yields of other particles, in particular of the ϕ meson. At intermediate e^+e^- invariant masses, we find a strong enhancement of the pair yield over a reference spectrum from elementary nucleon-nucleon reactions, suggesting the onset of nontrivial effects of the nuclear medium. Transverse-mass spectra and angular distributions have been reconstructed in three invariant mass bins. In the former unexpectedly large slopes are found for high-mass pairs. The latter, in particular the helicity-angle distributions, are largely consistent with expectations for a pair cocktail dominated at intermediate masses by Δ Dalitz decays.

PACS number(s): 25.75.Dw, 13.40.Hq

---

*Also at ISEC Coimbra, Coimbra, Portugal.

†Also at ExtreMe Matter Institute EMMI, D-64291 Darmstadt, Germany.

‡Also at Technische Univesität Darmstadt, Darmstadt, Germany.

§Corresponding author: R.Holzmann@gsi.de

∥Also at Dipartimento di Fisica, Università di Milano, I-20133 Milano, Italy.

¶Also at Technische Universität Dresden, 01062 Dresden, Germany.

**Now at Lawrence Berkeley National Laboratory, Berkeley, California, USA.

††Now at Dipartimento di Fisica Generale, Università di Torino, I-10125 Torino, Italy.

I. INTRODUCTION

Lepton pairs emitted from the hot and dense collision zone formed in heavy-ion reactions are appropriate probes for investigating in-medium properties of hadrons and, in general, the properties of hadronic bulk matter under extreme conditions. In fact, according to theory, there is even the potential to detect new phases of nuclear matter in the laboratory by isolating their telltale signals, among which are the direct decays of the short-lived vector mesons into e^+e^- or $\mu^+\mu^-$ pairs [1]. Indeed, the electromagnetic current-current correlator, which enters into the virtual photon emission rate [2], depends on the properties of the strongly interacting medium and its constituents [3].

Dilepton spectra measured by the CERES [4] and NA60 [5] experiments at CERN-SPS energies ($40A$–$158A$ GeV) pointed to a significant in-medium modification of the ρ meson spectral function, as signaled by a large additional yield (excess) of lepton pairs in the invariant mass region below the ρ meson pole mass. At the much lower beam energies of $1A$–$2A$ GeV the DLS [6] collaboration at the Bevalac observed a similar dielectron excess over the "hadronic cocktail," that is, the cocktail resulting from meson decays in the late (freeze-out) phase of the collision. However, in contrast to the situation at higher energies, for a long time this excess could not be satisfactorily explained by theoretical models and became the so-called "DLS puzzle." The baryon-rich regime probed at low beam energies obviously requires a different theoretical treatment than the pion-dominated SPS regime.

The excess of electron pairs observed by DLS in the η mass region has recently been reinvestigated with the HADES[1] detector [7] at SIS18 with carbon beams of $1A$ and $2A$ GeV bombarding carbon targets [8,9]. These new data fully confirmed the earlier DLS result and thereby rechallenged theory to come up with a proper description of pair production at low energies. Comparing the excitation function of the excess pair multiplicity with the known π^0 and η meson production [10–12] revealed that the excess scales with bombarding energy very much like the pion yield does, but not at all like the η yield. This finding already suggested baryonic resonances—and mainly the $\Delta(1232)$—as a possible source of the e^+e^- excess yield.

Besides the role played by baryon resonance decays, also a strong virtual bremsstrahlung contribution to the pair yield from mainly $n + p$ interactions had been predicted in various microscopic model calculations [13–16]. Evidently, a good understanding of the $pp \to ppe^+e^-$ and $np \to npe^+e^-$ channels is required for a firm interpretation of dielectron emission from heavy-ion collisions. First data on dilepton production in nucleon-nucleon collisions had again been obtained by DLS [17], although with limited mass resolution and, at the lowest beam energies, limited statistics. Initial attempts to describe those results were based on the soft photon approximation [13], followed later by more involved calculations using the one-boson exchange (OBE) approach [14–16]. OBE models include contributions from a number of diagrams which add up coherently, leading to subtle, but sizable, interference effects in the cross sections of both $n + p$ and $p + p$ reactions. Moreover, extending those results to the description of heavy-ion reactions, for example, in the framework of transport models, is a very difficult task which is at present not yet fully mastered.

On the experimental side, things moved again when HADES started to study $p + p$ and $d + p$ interactions at $E_{kin} = 1.25A$ GeV, that is, just below the free η meson production threshold. The main goal of these experiments was to understand the $n + p$ bremsstrahlung contribution to e^+e^- production and to establish an experimental cocktail of dielectrons from "free" hadron decays at SIS18 energies. Using a deuterium beam, the "quasifree" $np \to npe^+e^-$ reaction was

therein tagged by the detection of a forward-going spectator proton. A comparison of these data with our former $^{12}C + ^{12}C$ result showed that pair production in the light C + C system can be understood as resulting from a mere superposition of free $N + N$ collisions [18]. Moreover, the excess pair yield in the C + C system, when normalized to the pion multiplicity, turned out to be largely independent of bombarding energy in the range of $1A$ to $2A$ GeV, thus providing us with a useful reference spectrum. Note also that very recent OBE calculations [19] come very close to describing the HADES $p + p$ and $n + p$ data consistently.

The questions now arising include the following. How does the pair yield evolve with increasing system size? Does the influence of the hadronic medium set in and, if yes, what are its characteristic signals? To address this complex we present here results from our measurement of e^+e^- production in the medium-heavy reaction system ^{40}Ar + KCl at $1.76A$ GeV in which we also have observed ω production for the first time at SIS18 bombarding energies. In Sec. II of this article a brief description of the experiment, as well as of the analysis procedures, is given. In Sec. III the reconstructed e^+e^- mass distribution is presented and its relevant features in terms of excess and vector-meson regions are discussed. In Sec. IV we show and discuss other pair observables: transverse-mass and angular distributions. Finally, Sec. V summarizes and concludes the paper.

II. THE Ar + KCl EXPERIMENT

The HADES detector operates at the GSI Helmholtzzentrum für Schwerionenforschung in Darmstadt with proton and heavy-ion beams being provided by the synchrotron SIS18. Technical aspects of the spectrometer are described in Ref. [7]; a schematic view is shown in Fig. 1. Here we recall that its main component serving for electron and positron identification (PID) is a ring-imaging Cherenkov detector (RICH). Further PID power is provided by (1) the time of flight measured in the plastic scintillator time-of-flight (TOF) wall, (2) the electromagnetic shower characteristics observed in the preshower detector, and (3) the energy loss signals from the four wire-chamber planes and the scintillators of the TOF wall. A 50-μm-thick segmented polycrystalline diamond detector (START) placed in front of the target provides the precise event time.

A beam of ^{40}Ar ions with a kinetic energy of $1.756A$ GeV was used for the Ar + KCl experiment discussed in this paper. The beam intensity was about 6×10^6 particles per 8-s spill. The fourfold segmented target was made of natural KCl with a total thickness of 5 mm, corresponding to 3.3% nuclear interaction length. The segmentation of the target (1.3% radiation length per segment) helped to minimize the conversion of photons into electron pairs in the target material. The four segments are indeed nicely visible in the reconstructed event vertex distribution along the z axis (i.e., beam axis) shown in Fig. 2.

The online event selection was done in two steps: A first-level trigger (LVL1) picked out those reactions in which the number of hits exceeded 16 in the TOF scintillators. In total,

---

[1]High Acceptance DiElectron Spectrometer.
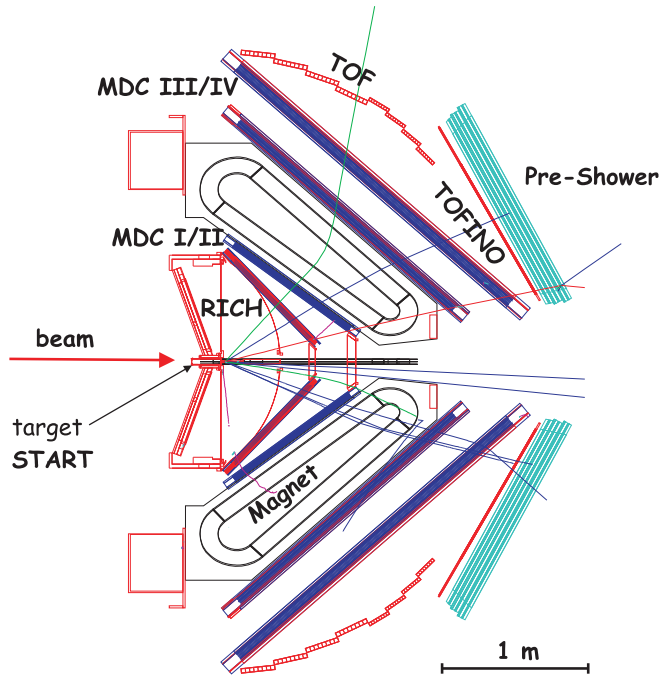
FIG. 1. (Color online) Schematic view of the HADES detector as implemented in the simulation. Simulated particle tracks are shown as well.

2.2×10^9 of such events were examined with a second-level trigger (LVL2) to find single lepton signatures of which about 6×10^8 were finally recorded. In the off-line analysis, events were further filtered by cutting on the event vertex reconstructed with a resolution of $\sigma_x = \sigma_y \simeq 0.4$ mm and $\sigma_z \simeq 1.9$ mm. These vertex cuts removed about 5% of the events
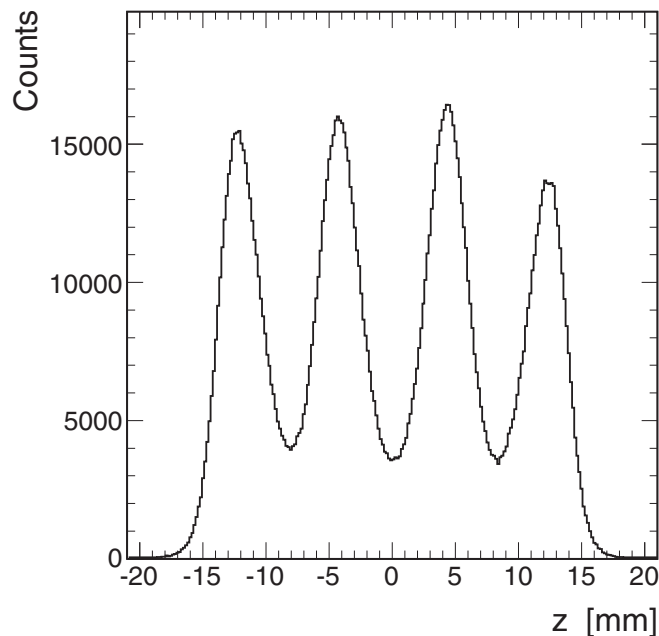

FIG. 2. Reconstructed event vertex distribution along the beam axis z. The four KCl target segments are clearly separated.

in accordance with the event rate observed in an empty-target run. The LVL1 trigger enhanced the mean pion multiplicity approximately two times with respect to the minimum-bias multiplicity. From our charged-pion analysis and a simulation of the trigger response to UrQMD events, we found that this corresponds to a mean number of participating nucleons of $\langle A_{\text{part}}^{\text{LVL1}} \rangle = 38.5$ and an average charged-pion multiplicity of $\frac{1}{2}(N_{\pi^+} + N_{\pi^-}) = 3.50 \pm 0.12(\text{stat}) \pm 0.22(\text{sys})$ (for details see Refs. [20,21]).

To investigate systematic effects in the dielectron reconstruction of the HADES experiment, three parallel data analyses were done with identification algorithms based, respectively, on (i) a multivariate analysis (MVA) [22,23], (ii) a Bayesian approach [7,24], and (iii) a combination of multidimensional selection cuts [7,25]. All three analyses led to consistent results with similar signal purities. The remaining differences were compounded with the other systematic uncertainties (see below). Identified electrons and positrons were further combined into pairs. The total number of reconstructed e^+e^- pairs, N_{+-}, can be decomposed as $N_{+-} = S + CB$, where S denotes the number of signal pairs and CB stands for the number of combinatorial background pairs. The former are the correlated e^+e^- pairs originating from the same parent particle and the latter ones are attributable to combining uncorrelated leptons stemming from separate sources, mostly π^0 Dalitz decays and external photon conversion. To reduce the CB, and hence enhance the S/CB ratio, it is, in particular, necessary to suppress contributions from photon conversion, from tracking fakes, and from misidentified hadrons. The main source of photons are the neutral-pion decays, $\pi^0 \to \gamma\gamma$. As the induced conversion pairs have mostly small opening angles, they have been effectively decimated with an opening-angle cut requiring $\alpha_{e^+e^-} \geqslant 9°$ in the laboratory frame. Tracking fakes were suppressed by selecting only ring-track combinations of sufficient reconstruction and matching quality [7]. Additionally, a single-lepton momentum cut of 0.1 GeV/c $< p_e < 1.1$ GeV/c confined the fiducial acceptance to the region where the combined track reconstruction and lepton identification efficiency was at least 10%, but typically 30%–70%, while the contamination of the lepton sample by charged pions and protons stayed well below 20%.

Finally, to obtain the e^+e^- invariant mass signal, the remaining CB was subtracted from all reconstructed pairs in the following way: In the low-mass region $M_{ee} < 0.4$ GeV/c^2, where the correlated background from the π^0 two-photon decay followed by double conversion contributes most, the combinatorial background was determined using a method based on like-sign e^+e^+ and e^-e^- pairs emerging from the same event; that is, $CB = 2\sqrt{N_{e^+e^+} N_{e^-e^-}}$. For larger masses, however, where the statistics of like-sign pairs is poor, we used a mixed-event CB normalized to the like-sign CB [7]. The mixing was done between events belonging to the same event class in terms of the track multiplicity (five selections) and the target segment (four selections), that is, for a total of 20 event classes. This procedure was applied likewise to all other pair observables, in particular, the pair transverse momentum distribution.

The resulting invariant mass spectrum of the dielectron signal, corrected for the detector and reconstruction
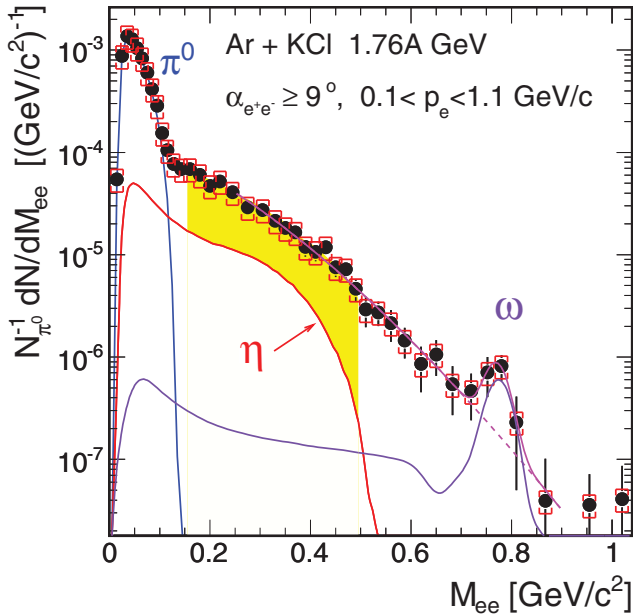
FIG. 3. (Color online) Reconstructed e^+e^- mass distribution in Ar + KCl collisions (averaged over three PID analyses, efficiency-corrected, CB subtracted, and normalized to N_{π^0}). Statistical and systematic errors of the measurement are shown as vertical bars and horizontal cups, respectively. Curves represent the π^0 and η Dalitz components, as well as the ω contribution (Dalitz and direct) simulated with the event generator Pluto. Also shown are the excess yield over the simulated cocktail (shaded area) and a fit (exponential + Gaussian curves) to the data in the mass range 0.25–0.9 GeV/c^2 (see Sec. III C for details).

inefficiencies,[2] but not acceptance, is shown in Fig. 3. The spectrum is normalized to the average number of charged pions—also measured in HADES [20]—namely, $(N_{\pi^-} + N_{\pi^+})/2 = 3.5$ per LVL1 event. As expected from isospin symmetry, this average is a good estimate of the actual π^0 yield N_{π^0}; that is, we set $N_{\pi^0} = (N_{\pi^-} + N_{\pi^+})/2$. The normalization to N_{π^0} compensates in first order the bias caused by the implicit centrality selection of our LVL1 trigger. The spectrum shown represents an averaged result from the three parallel PID analyses mentioned above. Besides the statistical error bars systematic errors are represented as horizontal ticks. They cover systematic effects attributed to the efficiency correction and combinatorial background subtraction (20%), to the error on the normalization (11%), and to differences between the three PID methods (10%). Statistical errors are, of course, point to point, the normalization error is global, and the remaining systematic errors are slowly varying with pair mass. The systematic errors given are upper bounds and add quadratically to 25%.

III. RESULTS FROM Ar + KCl

Here we discuss in more detail the efficiency-corrected and CB-subtracted dielectron invariant mass spectrum from Ar + KCl (see Fig. 3). The total yield of $\simeq 85\,000$ signal pairs is distributed over three easily distinguishable regions: (i) masses below 0.15 GeV/c^2, dominated by the π^0 Dalitz peak, contribute around 70 000, (ii) the intermediate range of 0.15–0.5 GeV/c^2 where the pair excess is located, holds about 15 000, and (iii) masses above 0.5 GeV/c^2 where the dileptons from vector meson decays are expected, total a few hundred pairs only ($\simeq 450$). All pair observables presented below have been obtained from inclusive LVL2-triggered events, that is, with no further centrality cuts. An investigation of different event classes selected by analysis cuts on the hit multiplicity revealed indeed a slight dependence of the normalized pair yields on centrality. However, as in this still rather small reaction system only a limited range of A_{part} can be scanned via such multiplicity cuts, we discuss below the A_{part} dependence only in the context of a comparison of Ar + KCl with C + C.

A. Low-mass pairs

The low-mass region contains the bulk of the pair yield, but it is also the one most strongly affected by the momentum-dependent efficiency corrections. As more than 90% of this yield stems from the π^0, it offers a convenient handle for validating our dielectron reconstruction and normalization procedures. To do this check we simulated the pion and η contributions to the e^+e^- cocktail with the Pluto event generator [26,27] using the meson multiplicities and source parameters given in Table I. In case of the π^0 they were taken from our own charged-pion data [20,21], in case of the η they were interpolated from Two-Arm Photon Spectrometer (TAPS) measurements of 1.5A and 2.0A GeV Ar + Ca (Ca + Ca) reactions [11,12]. Note that for both mesons a two-slope parametrization has been used. The validity of this interpolation is confirmed in Fig. 4, where π^0 and η midrapidity $1/m_\perp^2\, d^2N/dm_\perp\, dy$ spectra from TAPS are compared with the corresponding π^+ and π^- average measured in Ar + KCl [20] (midrapidity $y_0 = 0.858$ and $|y - y_0| < 0.1$). In this figure, the different centrality selections of the TAPS (minimum bias) and

TABLE I. Thermal source parameters used in the Pluto simulation of the dielectron cocktail. For all listed particles we give the multiplicity (N) within our LVL1 trigger condition, the source temperatures (T_1 and T_2), the relative strength (frac = $c_1/(c_1 + c_2)$, where c_1 and c_2 are the amplitudes of the two components) of the first component, the polar anisotropy (A_2), and the helicity coefficient (B) of the dielectron decay (see Sec. III E).

Particle	N	T_1 (MeV)	T_2 (MeV)	frac	A_2	B
π^0	3.5	52	89	0.85	0.75	1
η	8.8×10^{-2}	52	89	0.85	0.75	1
$\Delta^{+,0}$	$3\,N(\pi^0)$	80	—	1	0.75	1
ω	6.7×10^{-3}	80	—	1	0.75	0
ρ	5×10^{-2}	80	—	1	0.75	0
ϕ	2.6×10^{-4}	80	—	1	0.75	0

---

[2]Inefficiencies were determined with an event overlay technique in which simulated lepton tracks were embedded into real events, reconstructed, and tallied.
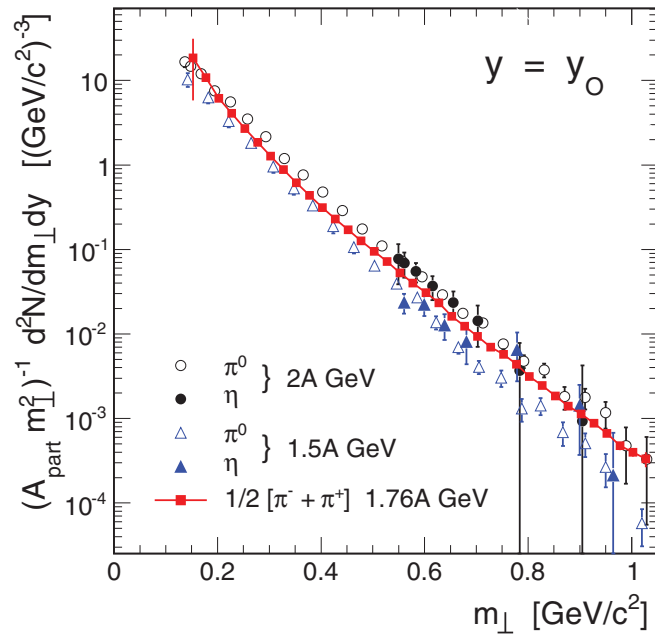
FIG. 4. (Color online) Average of the midrapidity charged-pion $d^2N/dm_\perp dy$ distributions, $N = 1/2[N_{\pi^+} + N_{\pi^-}]$, measured with HADES in the 1.76A GeV Ar + KCl reaction [20,21] (squares linked by solid curve), compared with the corresponding neutral pion and η data from 1.5A GeV ^{40}Ar + ^{nat}Ca and 2.0A GeV ^{40}Ca + ^{nat}Ca reactions obtained with the photon calorimeter TAPS [11,12] (circles and triangles). All yields are normalized to their respective $\langle A_{part} \rangle$; error bars shown are statistical.

HADES (LVL1) experiments are compensated by normalizing to the mean number of participating nucleons $\langle A_{part} \rangle = 20$ and 38.5, respectively. The Ar + KCl charged-pion average falls nicely in between the neutral pion (and η) data, as expected from the smooth beam energy dependence of pion production. The characteristics of the vector meson sources (ρ, ω, ϕ) are still largely unknown and have tentatively been set as given in Table I.

Turning back to Fig. 3, one can see that the low-mass pair yield is indeed described very well by our calculation, lending confidence to the reconstruction process.

B. Intermediate-mass excess

Comparing a Pluto simulation of long-lived sources (i.e., emitting mostly after freeze-out) with the data in Fig. 3 reveals that also in Ar + KCl the contributions from η (and ω) Dalitz decays do not exhaust the measured pair yield at intermediate masses, that is, for $M_{ee} \simeq 0.15$–0.5 GeV/c^2. Just like in our previous C + C measurements [8,9], there is a strong excess over the cocktail of known long-lived sources. We know furthermore from our comparison [18] of dielectron production in free nucleon-nucleon and C + C reactions that in the light carbon-carbon system the excess yield N_{exc} is of baryonic origin: Δ decays and NN—that is, mostly pn—bremsstrahlung. The C + C reaction seems to be in first order an incoherent superposition of elementary NN processes. In addition, whereas between 1A and 2A GeV η

production increases steeply with bombarding energy (from subthreshold to above threshold), the excess yield rises like pion production, that is, only mildly. This means that our isospin-averaged $\frac{1}{2}[pp + np]$ pair spectrum measured at 1.25 GeV [18] can serve as NN reference for the η-subtracted pair yield observed in the present 1.76A GeV Ar + KCl run as well, both normalized to their respective π^0 multiplicity. Note, however, that this reference is, of course, available only up to its kinematic cutoff at $M_{ee} = 0.55$ GeV/c^2, corresponding to the 1.25-GeV bombarding energy used in the NN experiments.

Figure 5 (top) shows the Ar + KCl e^+e^- invariant-mass distribution after subtracting the simulated η component and normalizing to N_{π^0}, together with the NN reference from Ref. [18] (adjusted to the acceptance, that is, magnetic field and momentum cuts, of the present experiment), also η subtracted and normalized to its π^0 multiplicity (averaged from $p + p$ and $p + n$ data). In this comparison we do not correct for the slight isospin asymmetry of the Ar + KCl system ($N/Z = 1.15$). Owing to the normalization and the use of a common acceptance both distributions agree in the π^0 Dalitz peak. They differ, however, strikingly for masses between 0.15 and 0.5 GeV/c^2, where the yield from the heavy system exceeds the NN reference by a factor of $\simeq 2.5$–3. This is also visible in the lower part of Fig. 5, where the ratios of the following pair yields are shown: Ar + KCl/$N + N$, and C + C/$N + N$ for 1A and 2A GeV. For this the C + C data were taken from [8,9] and transformed into the acceptance of the present experiment. The Ar + KCl/$N + N$ ratio is very close to unity at low masses, dominated by the π^0 Dalitz pairs, but for $M > 0.15$ GeV/c^2 it rises to about 3, indicating the onset of processes not accounted for in the reference system. Both representations prove that a qualitative change happens in the nature of the excess yield when going to the heavier system. Consequently, in contrast to the C + C system, Ar + KCl cannot anymore be seen as a superposition of independent $N + N$ collisions. A more complex picture involving multibody and multistep processes and maybe even in-medium modifications of the involved hadrons is required. Note also that a scaling with the number of binary nucleon-nucleon collisions N_{coll} might be more appropriate to describe the observed variation of the excess yield with system size. Indeed, $\langle N_{coll} \rangle$ calculated within a Glauber approach [28] increases faster than $\langle A_{part} \rangle$ when going from our LVL1 C + C to LVL1 Ar + KCl events, namely by a factor 6.1 for $\langle N_{coll} \rangle$ vs 4.5 for $\langle A_{part} \rangle$.

Combining the dielectron results from HADES and from the former DLS experiment we can now study the evolution of the excess over cocktail with beam energy *and* system size. To do so we have compiled in Fig. 6 the excess yields integrated over the mass region $M_{ee} = 0.15$–0.5 GeV/c^2 from all available reaction systems [6,8,9]. For comparison, inclusive π^0 and η multiplicities measured in photon calorimetry with the TAPS detector [10,11] are plotted as well. Note that all yields are extrapolated to the full solid angle[3] and are normalized to their

---

[3]Assuming similar geometric acceptances for excess pairs and η Dalitz pairs.
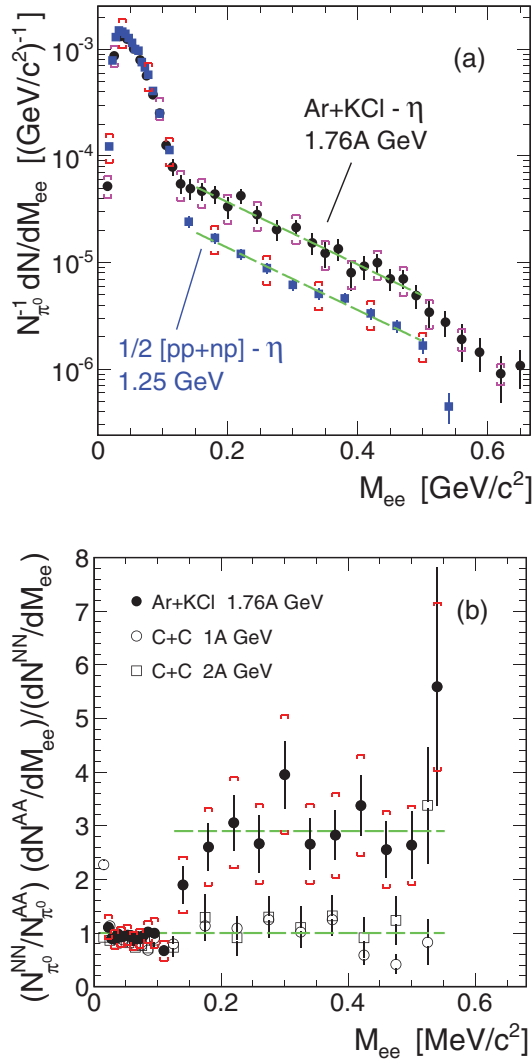
FIG. 5. (Color online) (a) Comparison of the Ar + KCl invariant-mass distribution with an isospin-averaged reference from $p + p$ and $n + p$ data [18]. For clarity systematic error bars are shown only on every second data point (vertical bars are statistical; cups are systematic). Both data sets are normalized to their respective pion multiplicity and have their respective η Dalitz yield subtracted. The dashed lines are meant to guide the eye. (b) Ratio of the heavy-ion mass distributions (Ar + KCl and C + C) to the 1/2 [$pp + np$] reference, whose total error (statistical and systematic added quadratically) is indicated by the shaded band. Note that all data sets are shown within the acceptance of the Ar + KCl experiment.

respective average A_{part} in order to compensate for differences in the centrality selection of the various experiments. The normalization also takes out the trivial system-size dependence of the yields, as visible from the closeness of the C + C and Ca + Ca meson curves.[4] The somewhat smaller pion multiplicity per A_{part} of Ca + Ca can be attributed to meson

----

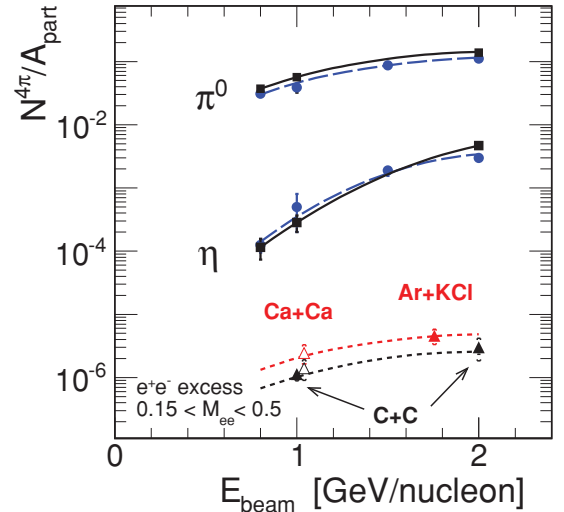[4]We consider here the systems Ar + KCl and Ca + Ca as being equivalent in size and isospin.

FIG. 6. (Color online) Inclusive multiplicity per participant, $N^{4\pi}/\langle A_{\text{part}}\rangle$, as function of beam energy of the e^+e^- pair excess over the η Dalitz yield, and of π^0 and η production in heavy-ion reactions. The excess yield, defined in the mass range $M_{ee} = 0.15$–0.5 GeV/c^2 and extrapolated to 4π, is shown for HADES Ar + KCl and C + C data (solid triangles) [8,9] as well as for DLS data (open triangles) [6]. The π^0 and η results are from TAPS measurements in C + C (squares, solid curves) and Ca + Ca (circles, long-dashed curves) collisions [10,12]. The curves are polynomial fits to these data used to interpolate the multiplicities as a function of bombarding energy (see [11]). For easier visual comparison with the energy dependence of the dielectron excess the latter is overlaid with the π^0 curves (short-dashed) downscaled by factors of 1.8×10^{-5} for C + C and 4.3×10^{-5} for Ar + KCl.

re-absorption in this larger system. Note, however, that the η multiplicities start out with the opposite behavior at low beam energy and switch only around $E_{\text{beam}} = 1.5A$ GeV to the absorption-dominated scaling. This crossing can be explained by the transition from the subthreshold regime, where multistep processes favored by a larger reaction volume are important [29], to above threshold production.

Next one can see that the dielectron excess follows pion production with rising bombarding energy, as we stated already before [8]. This turns out to be true for both the C + C and Ca + Ca collision systems, as one can see from the excellent match with the scaled-down pion production curves in the figure. Such a behavior has been interpreted as being characteristic of a production mechanism not driven by the excitation of heavy resonances, but rather by low-energy processes like pion production and propagation involving the Δ and, maybe, low-mass ρ excitations, as well as bremsstrahlung [18].

As already pointed out, the systematics of excess yields has become sufficiently rich to allow also for a study of the system-size dependence of the electromagnetic radiation from the nuclear medium. Above we concluded that the comparison of the excess yield obtained in Ar + KCl with the NN reference reveals a nontrivial behavior of pair production. This is also supported by Fig. 6, where an increase of a factor $\simeq 2$ is visible when moving from the C + C to the Ca + Ca system. Evidently, the excess yield must scale faster than

linear with A_{part} in contrast to the behavior of, for example, pion production in heavy-ion reactions. The mass dependence can indeed be further quantified by adjusting a $N_{\text{exc}} \propto A_{\text{part}}^{\alpha}$ scaling law to the yields. Using the Ar + KCl excess obtained at 1.76A GeV and interpolating the C + C excess for that beam energy we get a coefficient $\alpha = 1.41_{-0.27}^{+0.19}$. Using instead the DLS point measured at 1.04A GeV results in a similar scaling coefficient. Note that, when varying $\langle A_{\text{part}} \rangle$ by comparing systems of different size, the corresponding scaling exponent for pion production has been found to be $\alpha \simeq 0.85$ [12,30], independent of beam energy, and the one for η production to be $\alpha \simeq 1.2$ at 1A GeV, decreasing to $\alpha \simeq 0.8$ at 2A GeV [12]. These numbers confirm that the dielectron excess scales with system size very differently than the freeze-out yields of pions and η mesons.

All of our observations put together may be interpreted as the onset multibody and multistep processes in the hot and dense phase created in collisions of nuclei of such a size. The penetrating nature of the dilepton probe offers then a natural explanation for the behavior of the excess e^+e^- yield if one keeps in mind that for a sufficiently large number of participating nucleons or, in other terms, for a sufficiently large collision volume the detected radiation is the integral over the full time of the complex heavy-ion reaction and not just a snapshot at freeze-out. It will be interesting to follow up on this trend when still heavier systems are added to the systematics.

C. High-mass pairs from ω decays

We turn now to the high-mass region of the invariant mass spectrum and, in particular, to the clearly protruding peak structure which we attribute to the direct decay, $\omega \to e^+e^-$, of the ω vector meson. A linear zoom-in onto the vector-meson region is shown in Fig. 7. The peak visible at the ω pole position holds about 40 reconstructed pairs, limiting, unfortunately, the extent to which one can possibly go in its analysis. These data constitute the very first observation of ω production in a heavy-ion reaction at such a low beam energy, in fact, an energy even below the production threshold in free $N + N$ collisions ($E_{\text{thr}}^{NN} = 1.89A$ GeV). One expects that most of the ω's contributing to this peak decayed after having left the reaction zone, that is, after freeze-out. Recently measured ω photoproduction cross sections [31–33] have been interpreted [1] in the sense of a strong broadening (up to 150 MeV) of the decay width of this meson in the nuclear medium already at normal nuclear density. We do not observe such a modification in our ω signal: the shape of the observed peak is solely determined by the detector response, that is, by the intrinsic momentum resolution of the HADES tracking system. In this mass region also ρ^0 decays and baryonic resonance decays are expected to contribute to the dielectron yield, but they add up to a broad continuum underneath the ω peak. For masses above 0.9 GeV/c^2 the statistics is running out quickly and there is no recognizable structure at the pole position of the ϕ meson ($M_\phi = 1.019$ GeV/c^2).

All of this justifies fitting the whole mass region with the sum of a Gaussian shape and an exponential function,
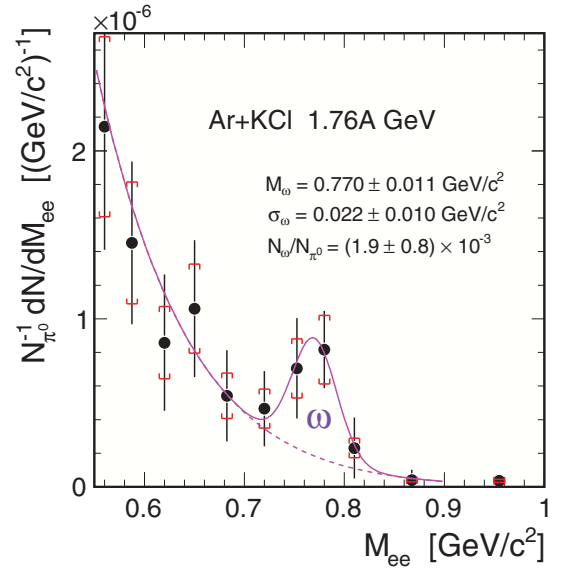

FIG. 7. (Color online) Zoom into the measured e^+e^- mass distribution in Ar + KCl (efficiency corrected and normalized), together with a least-squares fit of the ω vector meson peak by a sum of a Gaussian function and an exponential background (see text for details). Error bars are like in Fig. 3.

as shown in Fig. 7. The fit ($\chi^2/ndf = 11.8/18$) provides a peak position of $M_\omega = 0.770 \pm 0.011$ GeV/c^2, a width of $\sigma_\omega = 0.022 \pm 0.010$ GeV/c^2, and an integrated signal over the continuum corresponding to $(3.9 \pm 1.7) \times 10^{-8}$. The peak centroid agrees hence within about one standard deviation with the listed ω pole position at 0.783 GeV/c^2 [34]. Furthermore, detector simulations show that part of the observed downshift ($\simeq 10$ MeV) is attributable to the combined energy loss of the electron and positron in the inner part of the HADES detector. The peak width is dominated by the HADES mass resolution σ/M at the ω pole mass of 3%. Finally, its integral has been corrected for the branching ratio of the direct e^+e^- decay [34] as well as for the acceptance of 0.29 (obtained from a Pluto simulation done for a thermal source with a temperature of $T = 84 \pm 2$ MeV, as found in our $\phi \to K^+K^-$ analysis [35] for the ϕ meson). This resulted in a normalized yield of $N_\omega/N_{\pi^0} = (1.9 \pm 0.8) \times 10^{-3}$, corresponding to an ω LVL1 multiplicity of $M_\omega^{\text{LVL1}} = (6.7 \pm 2.8) \times 10^{-3}$. Fits with more sophisticated peak shapes taking into account the slightly asymmetric momentum response of the detector gave very similar results. The acceptance correction depends mildly on the phase-space distribution used in the Pluto simulation: It ranges from 0.34 at $T = 50$ MeV to 0.24 at $T = 140$ MeV (see also the discussion of the pair $m_\perp$ slopes in the next subsection). It depends even less on the assumed polar distribution: 5% decrease when varying A_2 from 0 to 1. All those effects are finally subsumed into an additional systematic error on the multiplicity of 25%. With the ω yield known, both its contributions—Dalitz and direct—to the pair cocktail can be simulated in Pluto; they are shown together with the mass spectrum in Fig. 3. The ω decays contribute evidently only a small part to the total pair yield at intermediate and low masses. Note finally that the average ω momentum

in the nucleus-nucleus center-of-mass within the HADES acceptance is found from our data to be $p = 0.43$ GeV/c. This is at least a factor of two smaller than the momenta typically observed in ω photoproduction experiments [31–33].

The ω multiplicity can be discussed in the context of either a scenario of complete thermalization at freeze-out or, in the other extreme, of production in elementary $N + N$ collisions. As HADES is a general-purpose charged-particle detector, besides the dielectron results presented here, a wealth of information has been obtained as well on hadron production in Ar + KCl. These findings have already been published in Ref. [20] on $\pi^{\pm}$, in Ref. [35] on K^+, K^-, and ϕ, in Ref. [21] on K_s^0, in Ref. [36] on Ξ^-, and finally in Ref. [37] on Λ and $\Sigma^{\pm}$.

In particular, from our $K^+ - K^-$ correlation analysis [35], a LVL1 ϕ multiplicity of $M_{\phi} = [2.6 \pm 0.7(\text{stat}) \pm 0.1(\text{sys})] \times 10^{-4}$ has been found, as well as a transverse-mass slope at midrapidity of $T_{\phi} = 84 \pm 8$ MeV. Together with the ω multiplicity, this gives a ϕ/ω ratio of $R_{\phi/\omega} = 0.043^{+0.050}_{-0.015}(\text{stat}) \pm 0.011(\text{sys})$. The experimental ratio can be compared to various predictions, running from pure $m_{\perp}$ scaling in 4π solid angle, giving $R \simeq 0.042$, to a full-fledged statistical hadronization model calculation performed with the THERMUS code [38] fitted to our hadron yields [37] and resulting in $R = 0.063 \pm 0.008$. Hence, statistical descriptions agree within error bars with the experimental $R_{\phi/\omega}$. As already discussed in Ref. [37], the THERMUS model does well in reproducing our measured hadron yields, including those of particles with open or hidden strangeness, with the notable exception of the double-strange Ξ^- which, however, at 1.76A GeV is produced far below its threshold of 3.57 GeV in free NN collisions.

The opposite extreme to complete thermalization is given by elementary $N + N$ and $\pi + N$ reactions, where the ϕ/ω ratio is traditionally investigated in the context of the so-called Okubo-Zweig-Iizuka (OZI) rule violation [39–41]. The ratio obtained in those reactions for small values of the excess energy ($\epsilon = E_{\text{c.m.}} - E_{\text{thr}}$) notoriously exceeds predictions based on the ϕ-ω mixing angle and is sometimes related to a possible $s\bar{s}$ admixture in the nucleon ground-state wave function. Figure 8 shows $R_{\phi/\omega}$ obtained in this work and the THERMUS value from a fit to HADES data together with results from elementary $p + p$ [42,43] and $\pi + N$ [44] reactions, all plotted as function of the excess energy in the $NN \rightarrow NN\phi$ and $\pi N \rightarrow N\phi$ reactions, respectively. This is different from the common definition in literature where the ϕ and ω yields are both taken at the *same* excess energy, corresponding hence to different bombarding energies, whereas we take the ratio of yields measured at a common beam energy. In fact, to do this, we divided the measured ϕ cross sections by an interpolation of the ω cross sections based on the parametrization proposed in Ref. [40] and, in case of the $p + p$ data, updated in Ref. [45]. One can see from the comparison that in the heavy-ion reaction the ratio $R_{\phi/\omega}$ is more than an order of magnitude larger than in NN collisions and also at least a factor 3–5 larger than in pion-induced processes. One should furthermore keep in mind that mostly low-momentum pions are produced in 1A–2A GeV heavy-ion reactions while the ϕ production threshold is at $p_{\pi} = 1.56$ GeV/c; in $N + N$ collisions the production threshold is at 2.60 GeV. Consequently, the
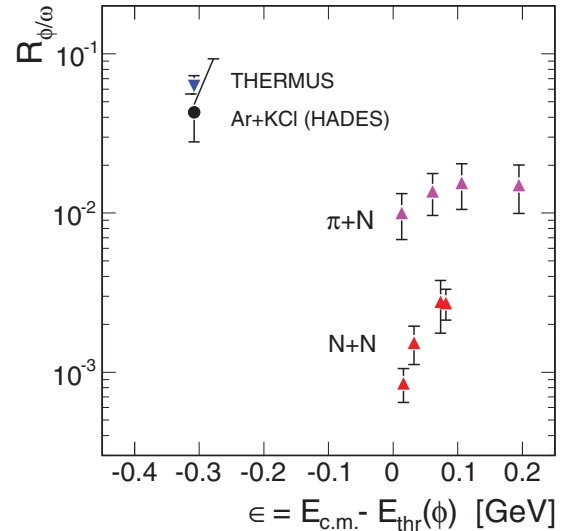

FIG. 8. (Color online) Comparison of the $R_{\phi/\omega}$ ratio obtained in this work with its statistical model (THERMUS fit) value as well as with a compilation of data from elementary $p + p$ and $\pi + N$ reactions (see text). The ratio is plotted as a function of the excess energy ϵ in the $NN \rightarrow NN\phi$ and the $\pi N \rightarrow N\phi$ reactions, respectively.

ϕ meson is produced subthreshold here ($\epsilon < 0$) and more complex, multistep processes involving short-lived resonances [46] and/or hyperons [47] might contribute. However, the ratio could also be influenced by final-state effects of the vector mesons in the nuclear medium (see, e.g., Ref. [1] for a discussion of ω and ϕ absorption). In the end, our observation seems to support the picture of meson production in a rather long-lived and thermalized fireball.

D. Dielectron $m_{\perp}$ distributions

We present now phase-space distributions of e^+e^- pairs in Ar + KCl. When discussing the pair mass spectrum (see Fig. 3) we distinguished different mass regions of interest. Indeed, the pair spectrum is a complicated cocktail emitted from various processes and at different phases of the heavy-ion reaction. As pointed out above, at low masses the situation is rather simple because this region is dominated by pairs from the π^0 Dalitz decay. In all other regions, however, multiple sources contribute and their disentanglement is not trivial. We have, fortunately, constraints on the η Dalitz yield from earlier TAPS measurements and now also on the ω Dalitz yield from our own analysis of the multiplicity of this particle (see discussion in Sec. III C).

To characterize the dielectron yield beyond its mass distribution one has to reconstruct other pair observables, in particular, its longitudinal and transverse phase-space population. The longitudinal dimension is usually covered by plotting rapidity density as function of rapidity, dN/dy, and the transverse one by plotting either $dN/dp_{\perp}$ or $dN/dm_{\perp}$ with $m_{\perp} = \sqrt{p_{\perp}^2 + M_{ee}^2}$ as function of $p_{\perp}$ or $m_{\perp}$. The thermal nature of a particle source can be best recognized by plotting either its $1/m_{\perp}^2 \, dN/dm_{\perp}$ distribution at $y = y_0$ or its $1/m_{\perp}^{3/2} \, dN/dm_{\perp}$ distribution integrated over all rapidities [48]. Indeed, in semilogarithmic representation and for $m_{\perp} \gg T$, both functions turn into a

straight line where the inverse-slope parameter T may be interpreted as the source temperature. In case of measuring dilepton pairs the situation is further complicated by the decay kinematics of the three-body Dalitz decays. Consequently, the exact nature of the parent distribution can be distorted in the observed e^+e^- distribution. Note that, in order to obtain meaningful slopes, these distributions have to be corrected not only for efficiency but also for acceptance including the detector geometry as well as momentum and opening angle cuts. As mentioned in the discussion of the ω multiplicity determination, the acceptance correction has been obtained from Pluto simulations of a full pair cocktail (with the source parameters listed in Table I), while varying its source parameters to quantify systematic effects. The pair acceptance has thereby been determined as a one-dimensional function of transverse mass, averaged over rapidity within a given mass bin, and vice versa. We have verified that this procedure gives results compatible with the more complex multidimensional correction as a function of mass, transverse momentum, and rapidity. The resulting normalized dN/dy and $dN/dm_\perp$ spectra are shown in Fig. 9 for pairs of $M_{ee} < 0.13$ GeV/c^2, together with the corresponding simulated spectra. This low-mass bin—being dominated by π^0 Dalitz yield—is described to better than 10% by our Pluto event generator, as seen from the overlayed histograms. This agreement further strengthens our confidence in the pion phase-space distribution used in the simulation as well as in our dielectron reconstruction procedures in general.

In the context of this analysis we have also done a careful investigation of the signal purity, as one might fear that particularly the high $m_\perp$ pairs could be contaminated by misidentified high-momentum hadron tracks and/or fake tracks. This purity study has been done with an event mixing technique and confirmed as well with full simulations of the reconstruction and particle identification. Indeed, while our lepton purity is, on average, better than 0.95, it decreases with increasing lepton momentum, resulting nonetheless in a dielectron purity which remains better than 0.7 up to $m_\perp$ values of 1.5 GeV/c^2. Note that hadron and fake impurities in the lepton sample lead to uncorrelated pairs only and thus increase the combinatorial background which is, of course, subtracted, as discussed in Sec. II. We have checked in simulations that the CB subtraction indeed removes these additional uncorrelated contributions.

To take advantage of our full pair statistics, we have opted to use the $1/m_\perp^{3/2}\, dN/dm_\perp = N_\circ \exp(-m_\perp/T)$ representation in our systematic investigation of the transverse momentum distribution for several bins of pair mass displayed in Fig. 10. With increasing pair masses contributions from η Dalitz, Δ (and N^*) Dalitz, bremsstrahlung, and finally ω, ρ^0 and (very few) ϕ decays are successively probed. Although the limited statistics of our data required rather wide bins, particularly for the highest masses, one can see a distinctive pattern emerge: As one progresses from low to higher M_{ee}, the slope of the pair transverse-mass spectra first remains approximately constant at T around 80 MeV, but when approaching the vector meson region, it rises steeply to reach a value as high as 130 MeV.
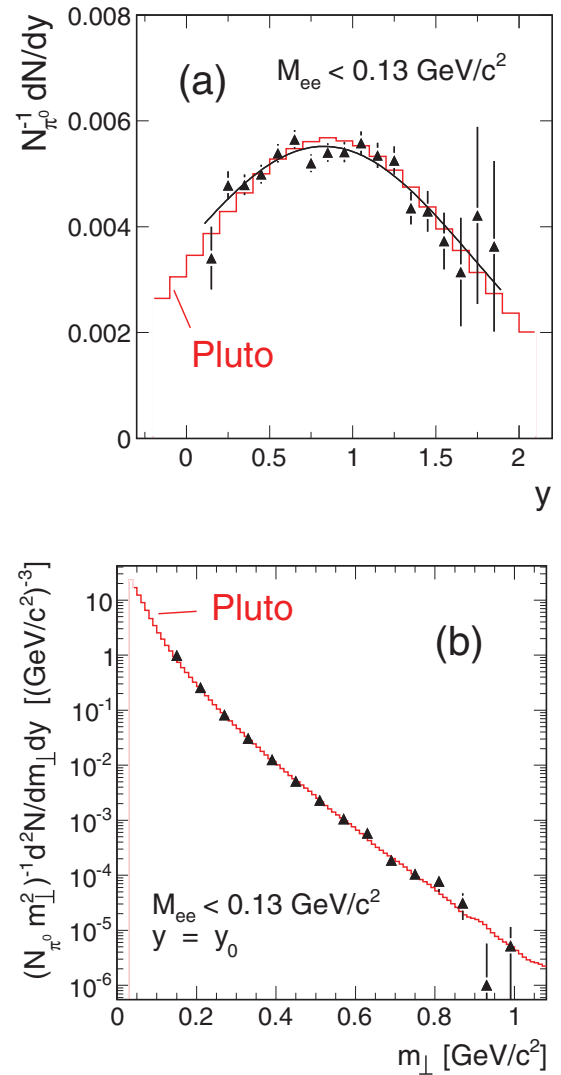

FIG. 9. (Color online) (a) Reconstructed rapidity and (b) transverse mass at midrapidity distributions of e^+e^- pairs with $M_{ee} < 0.13$ GeV/c^2. Data are normalized to N_{π^0} as well as corrected with the detector efficiency and acceptance. The error bars are statistical. The histograms correspond to a simulated (Pluto) cocktail of thermal sources. A Gaussian fit to dN/dy (top, solid curve), shown as well, results in $\langle y \rangle = 0.83 \pm 0.03$ and $\sigma_y = 0.91 \pm 0.07$.

While the first mass bin is dominated by π^0 Dalitz pairs, as emphasized in discussing Fig. 9, the next two bins cover the intermediate-mass region ($0.15 < M_{ee} < 0.5$ GeV/c^2), with contributions from η Dalitz, Δ Dalitz, NN bremsstrahlung, and maybe other sources. This is the region of the pair excess which we would like to characterize as much as possible. To do this, we have again subtracted the η component simulated with Pluto by making use of the known η multiplicity and source temperature. The resulting excess $dN/dm_\perp$ distribution is shown in Fig. 11 together with corresponding data obtained in C + C at $1A$ and $2A$ GeV, as well as with a reference from elementary nucleon-nucleon collisions, obtained from the average of our $p + p$ and $n + p$ results at 1.25 GeV [18], as discussed in Sec. III B. The spectrum from elementary $p + p$ collisions at 2.2 GeV [49] is also shown, but at this
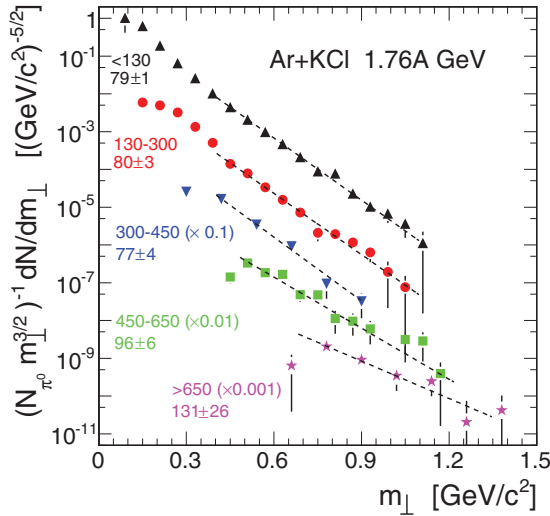
FIG. 10. (Color online) Reconstructed pair $1/m_\perp^{3/2}\,dN/dm_\perp$ distributions, normalized to the π^0 multiplicity, for the full rapidity range and different mass selections given in the left-hand side legends (in MeV). Efficiency and acceptance corrections are applied; error bars are statistical. Exponential fits to the high-$m_\perp$ region of the data are shown as dashed curves with the corresponding inverse-slope parameter given (in MeV) in the second line of the legends. Note also the scaling factors (in parentheses).

energy, unfortunately, the corresponding $n + p$ yields needed for isospin averaging are not available. All distributions are normalized to their respective neutral pion multiplicity, N_{π^0}, and have their respective η Dalitz contribution subtracted.[5] The figure shows that—within error bars and up to $m_\perp \simeq 0.5$, respectively, $\simeq 0.8$—the light C + C system behaves at both bombarding energies very much like the NN reference:

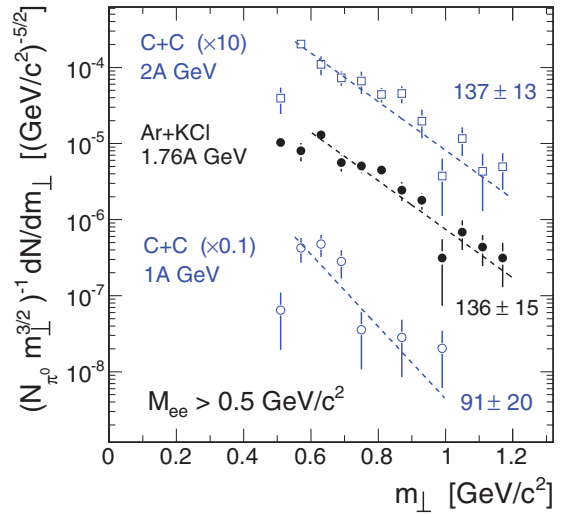[5]For 2.2 GeV $p + p$ only the exclusive η production has been subtracted.

FIG. 12. (Color online) Comparison of dielectron $1/m_\perp^{3/2}\,dN/dm_\perp$ distributions with $M_{ee} > 0.5$ GeV/c^2 and $-\infty < y < \infty$ in Ar + KCl and C + C (see text for details). Efficiency and acceptance corrections are applied. The distributions are normalized to the respective reaction pion yield N_{π^0}. Error bars are statistical. Dashed lines are exponential fits, with their corresponding inverse slope parameter given in MeV. Note also the scaling factors.

Normalized yields and slopes agree to a large extent. Note again that the reference spectrum can have yield only up to its kinematic cutoff at $m_\perp = 0.55$ GeV/c^2 (0.89 GeV/c^2 for 2.2 GeV $p + p$). In contrast to C + C, however, the Ar + KCl system displays a large excess over the elementary reference, just as found already in the comparison of the pair invariant mass spectra.

Moving finally to the large kinetic slopes found in the two upper mass bins, we note that this observation is surprising and difficult to reconcile with the assumption of a completely thermalized particle source. As one moves away from the
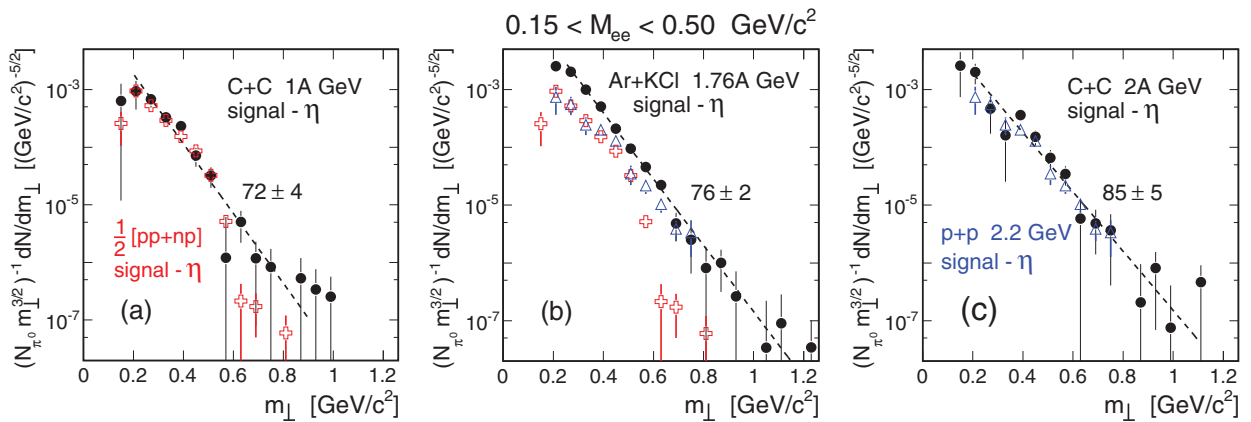

FIG. 11. (Color online) Reconstructed $1/m_\perp^{3/2}\,dN/dm_\perp$ distributions of pairs with $0.15 < M_{ee} < 0.5$ GeV/c^2 and $-\infty < y < \infty$ in C + C at 1A GeV (a), in Ar + KCl at 1.76A GeV (b), and in C + C at 2A GeV (c). Reference spectra from elementary NN collisions are also shown, namely, the average of $p + p$ and $n + p$ at 1.25 GeV (open crosses), and $p + p$ at 2.2 GeV (open triangles). Efficiency and acceptance corrections are applied. All distributions have their respective η contribution subtracted and are normalized to their respective pion multiplicity N_{π^0}. Error bars are statistical. Dashed lines are exponential fits, with the corresponding inverse slope parameter given in MeV.

three-body decays dominant below the η Dalitz edge at 0.547 GeV/c^2, the two-body decays of the vector mesons contribute more and more, and one expects indeed an increase of the slope parameter. This is just a natural consequence of the decay kinematics. However, from our THERMUS fit to the full set of hadron yields measured in Ar + KCl, we have found a chemical freeze-out temperature of the fireball of 76 MeV (see Sec. III C and Ref. [37]) and kinetic slope parameters in the range of 70–95 MeV [37], that is, of similar magnitude. In particular, the slope at midrapidity of the ϕ meson was found to be 84 ± 8 MeV in the K^+K^- channel [35]. Unfortunately, our statistics is not large enough to allow a tight selection around the ω pole mass and thus obtain the slope for a clean ω sample. From transport calculations [50] we estimate that the pair cocktail selected by our uppermost mass window (0.65–1.2 GeV/c^2) contains sizable contributions from the vector mesons ρ, ω, and ϕ, but its true composition remains of course uncertain.

Analyzing furthermore the corresponding $m_\perp$ slopes from the data sets of the C + C system [8,9] and comparing them with the present Ar + KCl result (see Fig. 12), we find a comparatively large slope in the light C + C system at $2A$ GeV. At the lower beam energy of $1A$ GeV, however, the C + C slope is found to be much smaller, but still large when compared with the 58-MeV slope of charged pions observed in this system [51].

Presently, we can only speculate about various effects that can lead to such a behavior of the transverse mass distributions. For example, collective effects, like radial flow, produce large effective temperatures and, in fact, yield slopes increasing with particle mass. However, such a trend is not visible in the systematics of kinetic slopes that we observed in Ar + KCl [37] and, moreover, in this rather small system the radial flow is not expected to be important [52]. Another mechanism that has been proposed is linked to the final-state interactions of the produced vector mesons. Indeed, if these interactions are strongly momentum-dependent, they can modify the spectral distributions. This has also been proposed as an explanation for the depletion of ω yield observed at low $p_\perp$ in In + In collisions by the NA60 experiment at the CERN-SPS [53]. Reabsorption cross sections of the ω meson in cold nuclear matter have been calculated in a OBE approach by the authors of Ref. [54] and they found them indeed large and strongly momentum dependent. Inserting these cross sections into transport calculations, they also predicted observable effects in the transverse-mass spectra of ω produced in heavy-ion collisions. Note that reabsorption of the vector mesons is closely related to their collisional broadening in the nuclear medium. From recent measurements of the transparency ratios in ω [32,55] and ϕ [56] photoproduction the collisional broadening of both mesons has been found to be quite large (at $\rho = \rho_0$, $\Gamma_\omega = 100$–150 MeV), although its exact momentum dependence could not yet be sufficiently constrained (see Ref. [1] for a discussion). Yet other factors that might influence the shape of the pair transverse mass distribution are the spectral functions of the various dilepton sources contributing. In particular, any enhancement at large masses owing to increased form factors, as predicted, for example, for resonance decays within vector-dominance models [57,58], could lead

to spectral distortions transcended in their characteristic $m_\perp$ slopes. To conclude, the interpretation of the large dielectron slope parameters observed in our heavy-ion data remains challenging.

E. Dielectron angular distributions

Angular distributions of the emitted dielectrons constitute yet another observable of interest. Various emission angles can be reconstructed. Here we focus on two specific ones: (i) the center-of-mass polar angle $\theta_{\mathrm{c.m.}}$, that is, the angle between the direction of the virtual photon in the $A + A$ reference frame and the beam axis, and (ii) the so-called helicity angle α, that is, the angle between the direction of the virtual photon in the reference frame of the mother particle (e.g., π^0, η, Δ for the three-body Dalitz decays and the fireball for the two-body direct decays) and the direction of the electron (or positron) in the pair frame. This particular choice of the latter angle corresponds to its definition in the so-called Jacob-Wick frame [59,60]. Technically, it requires a double Lorentz transformation of the lepton momenta: first from the laboratory frame into the parent particle frame and second from there into the virtual photon frame. Considering the decay kinematics, one can convince oneself that the polar angle of the dielectron will have at least reminiscence of the polar emission angle of the mother particle for three-body decays (i.e., Dalitz decays) and be equal to it in case of a two-body decay (i.e., vector meson $\rightarrow e^+e^-$). Likewise, the reconstruction of the helicity angle is exact only for two-body decays and approximate for three-body decays, because the third product goes undetected in the inclusive e^+e^- reconstruction we did. Nonetheless, our simulations show that these angular distributions are not completely attenuated if one makes the approximation that the decaying particle is at rest in the nucleus-nucleus center-of-mass frame and thus information can be gained on the parent particle and its decay. The amount of attenuation depends on the specific decay kinematics and on the source temperature of the mother particle.

The helicity distribution is of particular interest as it makes it possible to probe the degree of polarization of the virtual photon. It can be proven that pseudoscalar Dalitz decays are self-polarizing [61,62] and lead to helicity distributions of the form $dN/d\alpha \propto 1 + B\cos^2\alpha$ with $B = 1$, where α is the helicity angle. This expectation has been confirmed long ago for the π^0 in a study using the charge-exchange reaction $\pi^- p \rightarrow \pi^0 n$ [63] and again more recently in exclusive $p + p$ measurements at 2.2 GeV performed by the HADES collaboration [64]. This HADES measurement provided in addition the very first observation of the helicity distribution in η Dalitz decays. The simulations we have done to determine the sensitivity of our heavy-ion data to these effects reveal that the attenuation, caused by the incomplete reconstruction of the Dalitz decays, reduces the helicity anisotropy coefficient from unity to $B \simeq 0.6 - 0.7$ for $\pi^0 \rightarrow \gamma e^+e^-$ and $\eta \rightarrow \gamma e^+e^-$ decays, that is, leaving it still quite sizable. In case of the $\Delta \rightarrow N e^+e^-$ decay, the calculation of the helicity distribution is much more involved, but it has been done and likewise a distribution of type $1 + B\cos^2\alpha$ with $B \simeq 1$ is expected [65].

Exclusive dielectron data taken with HADES in 1.25-GeV $p + p$ collisions have also confirmed the latter prediction [66]. Finally, in the two-body decays—$\rho^0, \omega, \phi \rightarrow e^+e^-$—the dilepton simply carries the full polarization of the vector meson. Measuring helicity angles might hence help to unravel the different components of the pair cocktail [65,67–69]. These ideas have also been applied recently by the NA60 experiment to characterize the thermal nature of high-mass dimuon radiation emitted in high-energy heavy-ion reactions at the CERN-SPS [70].

Experimentally, the dielectron angular distributions are only obtained within the detector acceptance shown in Fig. 13, which they need to be corrected for. We have done this by dividing a given reconstructed polar distribution with a corresponding simulated cocktail distribution for which isotropic emission of the parent particle was assumed. Likewise, the experimental helicity distributions were divided by the corresponding simulated cocktail distribution assuming an isotropic emission of the decay lepton. From our simulations we expect that such a ratio, besides correcting for the acceptance, will reveal deviations of the data from isotropy. The π^0 dominated low-mass pairs can again serve as a test bed for the procedure. For these one expects to observe a polar distribution reminiscent of the known pion polar anisotropy [20], as well as the helicity distribution typical for pseudoscalar Dalitz decays, although attenuated. Figure 14
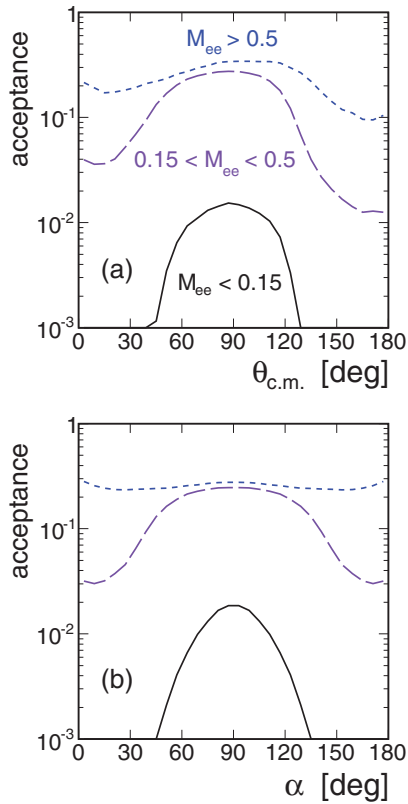

FIG. 13. (Color online) Acceptance of the HADES detector for the dielectron nucleus-nucleus center-of-mass polar emission angle $\theta_{c.m.}$ (a) and helicity angle α (b), represented for the three mass selections indicated in the figure.
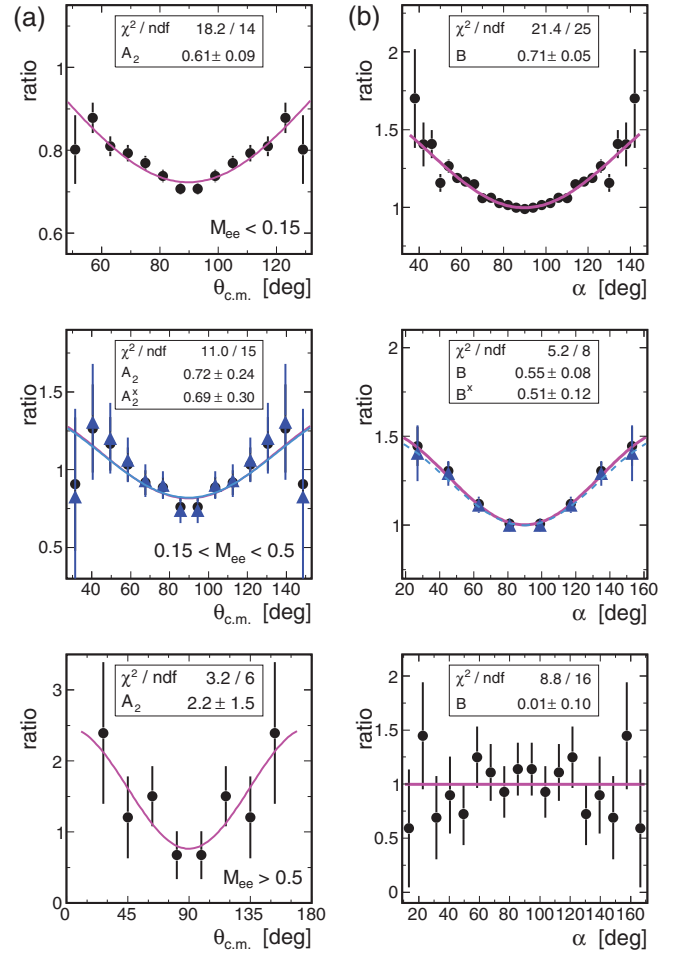

FIG. 14. (Color online) Ratio of measured and simulated dielectron center-of-mass polar distributions $dN/d\theta_{c.m.}$ (a) and helicity distributions $dN/d\alpha$ (b) for three mass bins: $M_{ee} < 0.15$, $0.15 < M_{ee} < 0.5$, and $M_{ee} > 0.5$ GeV/c^2 (from top to bottom). The error bars are statistical. The Pluto cocktail simulation was done assuming isotropic emission and decay of the dileptons (see text). The curves are fits to the data yielding the anisotropy coefficients, that is, polar A_2 and helicity B. The coefficients A_2^x and B^x result from fits (dashed curves) to the η-subtracted ratios (triangles).

shows the ratio of the reconstructed/simulated center-of-mass polar ($dN/d\theta_{c.m.}$) and helicity ($dN/d\alpha$) distributions for three different pair mass bins. Note that these ratios have been reflected about $90°$ and both halves added in order to reduce statistical fluctuations. The normalization is arbitrary. The resulting angular distributions exhibit anisotropies which are quantified by adjusting $1 + A_2 \cos^2 \theta_{c.m.}$ and $1 + B \cos^2 \alpha$ forms, respectively.

The low-mass anisotropies are large and consistent with our expectations for the neutral pion. The fitted polar coefficient $A_2 = 0.61 \pm 0.09$ corresponds, according to our simulation, to an unattenuated $A_2 = 0.76 \pm 0.11$, in agreement with the polar anisotropies of charged pions observed in Ar + KCl [20], namely, $A_2 = 0.75 \pm 0.05$. The helicity, $B = 0.71 \pm 0.05$, is attenuated by the thermal emission of the pion from its QED value $B = 1$, again consistent with the expectation from our simulations.

Intermediate-mass pairs are more interesting because only about 25%–30% of their yield is exhausted by η Dalitz pairs, the dominant excess part being of nontrivial nature (see discussion in Sec. III B). Angular distributions might provide some constraints on its possible composition. The intermediate-mass bin in Fig. 14 displays large anisotropies as well, both for polar emission angles, with $A_2 = 0.72 \pm 0.24$, and for helicity, with $B = 0.55 \pm 0.12$. Taking into account the attenuation, this is again compatible with the $1 + \cos^2 \alpha$ behavior typical for pseudoscalar meson, but also Δ decays. Subtracting the simulated η contribution from the data, the pure excess angular distributions have been obtained. They are represented as well in the figure, together with the corresponding fits, showing that the anisotropies ($A_2^x = 0.69 \pm 0.30$ and $B^x = 0.51 \pm 0.17$) of the excess yield turn out to be very similar to the ones of the η. This suggests that a large fraction of the excess can be attributed to decays of the Δ resonance for which indeed $B = 1$ is also expected. One has to keep in mind, however, that the nucleon-nucleon bremsstrahlung contributes as well in this mass region and has to be considered in a full description.

The high-mass bin is unfortunately very low in statistics, but exhibits nevertheless a strong polar anisotropy ($A_2 = 2.2 \pm 1.5$), whereas its helicity distribution is within its (large) statistical errors compatible with $B = 0$. This is to be expected if this mass bin contains large contributions from vector mesons emitted from a completely thermalized source, just like it was observed in the NA60 experiment [53], although this is in conflict with the observed large slope parameters.

IV. CONCLUSIONS AND OUTLOOK

The results on $e^+ e^-$ production obtained with HADES in the medium-heavy ^{40}Ar + KCl system at 1.756A GeV show an intermediate-mass pair excess over long-lived sources a factor 2–3 stronger than the one observed in elementary and ^{12}C + ^{12}C reactions. We have discussed the enhancement in the integral pair yields as well as differentially in the pair mass and transverse mass distributions. We have argued that this behavior signals the onset of influence of the nuclear medium on dilepton production. We have isolated the emission from the medium by subtracting the known contributions from long-lived pair sources. By presenting transverse mass and angular distributions of the η-subtracted yields, we have been able to characterize this contribution further. From the analysis of the excess transverse-mass slope and angular anisotropies we concluded that they are compatible largely with Δ Dalitz decays, suggestive of resonance matter.

Furthermore, for the first time at SIS18 energies, a clear ω signal could be observed in heavy-ion collisions, quantified, and compared with the prediction of a statistical hadronization model. This result allows, in particular, to put tight constraints on vector meson production in heavy-ion collisions at beam energies of a few GeV. From the shape and position of the observed peak no direct indications could, however, be found for medium modifications of this vector meson. In fact, in case of the very strong broadening of the ω implied by

the interpretation of photoproduction data, our measurement would anyhow have been sensitive only to the freeze-out, that is, vacuum part of its yield.

A first and preliminary comparison of our Ar + KCl invariant mass $e^+ e^-$ spectrum with predictions of models based on transport theory has been discussed in Refs. [50,71]. While both the hadron string dynamics (HSD) model [72] and the ultrarelativistic quantum molecular dynamics (UrQMD) model [73] achieve good agreement for invariant masses below 0.15 GeV/c^2, at intermediate and higher masses the description of the pair yield is not yet satisfactory. Known reasons are the still imperfect description of some of the elementary processes implemented in transport models, namely bremsstrahlung and vector meson production [18], but also the largely open question about how to treat possible in-medium modifications of these processes. However, these models suggest that the part of our spectrum most sensitive to possible in-medium modifications should be the region of excess yield, namely, the dielectrons with masses of 0.5–0.8 GeV/c^2, which hence need to be characterized in detail. With the additional and more differential $e^+ e^-$ data presented in this paper we have provided the information required to improve the theoretical description of dilepton production in heavy-ion collisions. Furthermore, once supplemented with data on yet heavier reaction systems, these new results are expected to reveal and quantify medium modifications of hadrons in warm and dense nuclear matter.

In summary, we have presented phase-space distributions (invariant mass, transverse mass, rapidity, polar angle, and helicity angle) of dielectrons for the reaction Ar + KCl at 1.756A GeV. From these the following results have been obtained: (i) observation of a strong excess (up to factor 3) over $N + N$ collisions of the pair yield at intermediate masses; (ii) first observation of ω production in heavy-ion collisions at such a low beam energy, yielding a ϕ / ω ratio consistent with maximal violation of OZI suppression; (iii) a systematic study of transverse-mass distributions with the observation of unexpectedly large inverse-slope parameters of up to 135 MeV, which might be related to final-state processes and/or the spectral functions of the contributing dilepton sources; and (iv) first exploitation of the virtual photon polarization observable at low beam energies.

Our studies on dielectron production in heavy-ion reactions will be pursued over the next years with an upgraded HADES detector [74], which will have the ability to handle the high track densities from truly heavy collisions, in particular also the ^{197}Au + ^{197}Au system. These data runs will thus provide the full systematics required to address open questions on the origin and properties of the intermediate-mass pair yield. In parallel to this heavy-ion program, the HADES experiment will also take up studies making use of the GSI secondary pion beams, in elementary $\pi + p$ reactions as well as in $\pi + A$ reactions. The pion-beam experiments will make it possible to conduct a comprehensive study of the contribution of specific baryon resonances to dielectron emission, in vacuum and in the nuclear medium. The information gained this way will, in turn, also help to improve our understanding of dilepton radiation from the hot and dense hadronic medium produced in the reactions with heavy ions.

[1] S. Leupold, V. Metag, and U. Mosel, Int. J. Mod. Phys. E **19**, 147 (2010).

[2] C. Gale and J. I. Kapusta, Nucl. Phys. B **357**, 65 (1991).

[3] B. Friman *et al.*, (Eds), *The CBM Physics Book*, Lecture Notes in Physics 814 (Springer, Berlin, 2011).

[4] D. Adamova *et al.* (CERES Collaboration), Phys. Lett. B **666**, 425 (2008).

[5] R. Arnaldi *et al.* (NA60 Collaboration), Phys. Rev. Lett. **96**, 162302 (2006).

[6] R. J. Porter *et al.* (DLS Collaboration), Phys. Rev. Lett. **79**, 1229 (1997).

[7] G. Agakishiev *et al.* (HADES Collaboration), Eur. Phys. J. A **41**, 243 (2009).

[8] G. Agakishiev *et al.* (HADES Collaboration), Phys. Lett. B **663**, 43 (2008).

[9] G. Agakishiev *et al.* (HADES Collaboration), Phys. Rev. Lett. **98**, 052302 (2007).

[10] R. Averbeck *et al.* (TAPS Collaboration), Z. Phys. A **359**, 65 (1997).

[11] R. Holzmann *et al.* (TAPS Collaboration), Phys. Rev. C **56**, R2920 (1997).

[12] R. Averbeck, R. Holzmann, V. Metag, and R. S. Simon, Phys. Rev. C **67**, 024903 (2003).

[13] C. Gale and J. I. Kapusta, Phys. Rev. C **35**, 2107 (1987).

[14] M. Schäfer, H. C. Dönges, A. Engel, and U. Mosel, Nucl. Phys. A **575**, 429 (1994).

[15] R. Shyam and U. Mosel, Phys. Rev. C **67**, 065202 (2003).

[16] L. P. Kaptari and B. Kämpfer, Nucl. Phys. A **764**, 338 (2006); Phys. Rev. C **80**, 064003 (2009).

[17] W. Wilson *et al.* (DLS Collaboration), Phys. Rev. C **57**, 1865 (1998).

[18] G. Agakishiev *et al.* (HADES Collaboration), Phys. Lett. B **690**, 118 (2010).

[19] R. Shyam and U. Mosel, Phys. Rev. C **82**, 062201 (2010).

[20] P. Tlustý *et al.* (HADES Collaboration), arXiv:0906.2309v1[nucle-ex].

[21] G. Agakishiev *et al.* (HADES Collaboration), Phys. Rev. C **82**, 044907 (2010).

[22] S. Lang, Ph.D. thesis, Frankfurt, 2008.

[23] Toolkit for MultiVariate Analysis with ROOT [http://tmva.sourceforge.net/].

[24] M. Jurkovic, Ph.D. thesis, München, 2010.

[25] F. Krizek, Ph.D. thesis, Prague, 2009.

[26] I. Fröhlich *et al.*, in *Proceeedings of XI International Workshop on Advanced Computing and Analysis Techniques*, Amsterdam (The Netherlands), 2007, PoS (ACAT) 076.

[27] F. Dohrmann *et al.*, Eur. Phys. J. A **45**, 401 (2010).

[28] M. L. Miller, K. Reygers, S. J. Sanders, and P. Steinberg, Annu. Rev. Nucl. Part. Sci. **57**, 205 (2007).

[29] A. R. Wolf *et al.*, Phys. Rev. Lett. **80**, 5281 (1998).

[30] W. Reisdorf *et al.* (FOPI Collaboration), Nucl. Phys. A **781**, 59 (2007).

[31] D. Trnka *et al.* (CBELSA/TAPS Collaboration), Phys. Rev. Lett. **94**, 192303 (2005).

[32] M. Kotulla *et al.* (CBELSA/TAPS Collaboration) Phys. Rev. Lett. **100**, 192302 (2008).

[33] M. Nanova *et al.* (CBELSA/TAPS Collaboration) Phys. Rev. C **82**, 035209 (2010).

[34] K. Nakamura *et al.* (Particle Data Group), J. Phys. G **37**, 075021 (2010).

[35] G. Agakishiev *et al.* (HADES Collaboration), Phys. Rev. C **80**, 025209 (2009).

[36] G. Agakishiev *et al.* (HADES Collaboration), Phys. Rev. Lett. **103**, 132301 (2009).

[37] G. Agakishiev *et al.* (HADES Collaboration), Eur. Phys. J. A **47**, 21 (2011).

[38] S. Wheaton and J. Cleymans, Comput. Phys. Commun. **180**, 84 (2009).

[39] A. I. Titov, B. Kämpfer, and B. L. Reznik, Phys. Rev. C **65**, 065202 (2002).

[40] A. Sibirtsev, Nucl. Phys. A **604**, 455 (1996).

[41] A. Sibirtsev and W. Cassing, Eur. Phys. J. A **7**, 407 (2000).

[42] F. Balestra *et al.* (DISTO Collaboration), Phys. Rev. C **63**, 024004 (2001).

[43] M. Hartmann *et al.* (ANKE Collaboration), Phys. Rev. Lett. **96**, 242301 (2006).

[44] A. Baldini, V. Flaminio, W. G. Moorhead, and D. R. O. Morrison, in *Landolt-Börnstein*, New Series, Vol. I/12a (Springer, Berlin, 1988).

[45] M. Abdel-Bary *et al.* (COSY-TOF Collaboration), Phys. Lett. B **647**, 351 (2007).

[46] H. Schade, Gy. Wolf, and B. Kämpfer, Phys. Rev. C **81**, 034902 (2010).

[47] E. E. Kolomeitsev and B. Tomasik, J. Phys. G **36**, 095104 (2009).

[48] R. Hagedorn, Suppl. Nuovo Cimento **3**, 147 (1965).

[49] B. Sailer, Ph.D. thesis, München, 2007.

[50] F. Krizek *et al.* (HADES Collaboration), Nucl. Phys. A **830**, 483c (2009).

[51] G. Agakishiev *et al.* (HADES Collaboration), Eur. Phys. J. A **40**, 45 (2009).

[52] W. Reisdorf *et al.* (FOPI Collaboration), Nucl. Phys. A **848**, 366 (2010).

[53] R. Arnaldi *et al.* (NA60 Collaboration), Eur. Phys. J. C **61**, 711 (2009).

[54] G. I. Lykasov, W. Cassing, A. Sibirtsev, and M. V. Rzjanin, Eur. Phys. J. A **6**, 71 (1999).

[55] M. H. Wood *et al.* (CLAS Collaboration), Phys. Rev. Lett. **105**, 112301 (2010).

[56] T. Ishikawa *et al.* (SPring8 Collaboration), Phys. Lett. B **608**, 215 (2005).

[57] M I. Krivoruchenko, B V. Martemyanov, A. Faessler, and C. Fuchs, Ann. Phys. **296**, 299 (2002).

[58] F. Iachello, Phys. Rev. C **69**, 055204 (2004).

[59] M. Jacob and G. C. Wick, Ann. Phys. **7**, 404 (1959).

[60] C. S. Lam and W. K. Tung, Phys. Rev. D **18**, 2447 (1978).

[61] N. M. Kroll and W. Wada, Phys. Rev. **98**, 1355 (1955).

[62] L. G. Landsberg, Phys. Rep. **128**, 301 (1985).

[63] N. P. Samios, Phys. Rev. **121**, 275 (1961).

[64] B. Ramstein *et al.* (HADES Collaboration), Acta Phys. Pol. B **41**, 365 (2010).

[65] E. L. Bratkovskaya, O. V. Teryaev, and O. V. Toneev, Phys. Lett. B **348**, 283 (1995).

[66] B. Ramstein *et al.* (HADES Collaboration), AIP Conf. Proc. **1257**, 695 (2010).

[67] E. L. Bratkovskaya, M. Schäfer, W. Cassing, U. Mosel, O. V. Teryaev, and O. V. Toneev, Phys. Lett. B **348**, 325 (1995).

[68] E. L. Bratkovskaya, W. Cassing, and U. Mosel, Phys. Lett. B **376**, 12 (1996); Z. Phys. C **75**, 119 (1997).

[69] T. I. Gulamov, A. I. Titov, and B. Kämpfer, Phys. Lett. B **372**, 187 (1996).

[70] R. Arnaldi *et al.* (NA60 Collaboration), Phys. Rev. Lett. **102**, 222301 (2009); (NA60 Collaboration), Eur. Phys. J. C **64**, 1 (2009).

[71] M. Jurkovic *et al.* (HADES Collaboration), *XLVIII International Winter Meeting on Nuclear Physics, Bormio 2010*, PoS (BORMIO2010) 051.

[72] E. L. Bratkovskaya and W. Cassing, Nucl. Phys. A **807**, 214 (2008).

[73] K. Schmidt, E. Santini, S. Vogel, C. Sturm, M. Bleicher, and H. Stöcker, Phys. Rev. C **79**, 064908 (2009).

[74] J. Pietraszko *et al.*, in *Annual Report 2010 of GSI Helmholtzzentrum för Schwerionenforschung*, Darmstadt (Germany).